two oligomers of different size that nevertheless contain the same quartet-forming guanine motifs. The number of independent products reveals the molecularity of the complex. Thus, if an equimolar mixture of the oligomers A and B (which contain the same G motifs, but are of different size) forms G4-DNA on appropriate treatment, then five different G4 products, corresponding to $A_4$, $A_3B$, $A_2B_2$, $AB_3$, and $B_4$, should form and be resolved in a nondenaturing gel.[18] Similarly a G′2-type complex should yield three product bands, corresponding to $A_2$, AB, and $B_2$.[17]

*Influence of pH and Melting of Refractory Quartet Structures*

G-quartet structures form within a fairly wide range of pH, centered around neutral. In general, pH 6.0–8.0 is found to be optimal. G4-DNA, once formed, is stable up to an alkaline pH of 12.0; however, at the acidic extreme, there exists a danger of depurination and precipitation. The alkali lability of G4-DNA above pH 12.0 may be exploited to denature complexes that are stable even to boiling in 90% formamide. To denature such a complex, (1) ethanol precipitate it and dry the pellet; (2) add 10 $\mu$l of ice-cold 25 m*M* NaOH, dissolve the DNA by vortexing, and store it on ice for 30 sec; and (3) neutralize the solution by promptly adding, in succession, 10 $\mu$l of 100 m*M* Tris, pH 7.0, and 10 $\mu$l of 25 m*M* HCl, vortexing briefly after each step to mix.

## [11] Parallel-Stranded Duplex DNA

*By* KARSTEN RIPPE and THOMAS M. JOVIN

### Introduction

A number of alternative DNA structures have been described in the literature in which some or all of the strands (2, 3, or 4 in number) have the same polarity, that is, a 5′–3′ orientation.[1] Most of these require modifications of the chemical structure of the DNA or certain solution conditions such as low pH. The parallel-stranded (ps) double helical structure denoted here as parallel-stranded DNA (ps-DNA) forms readily under physiological conditions and in the absence of chemical alterations of the bases or backbone, given the appropriate sequences.[1,2] The structural features of

[1] T. M. Jovin, *in* "Nucleic Acids and Molecular Biology" (F. Eckstein and D. M. Lilley, eds.), Vol. 5, p. 25. Springer-Verlag, Berlin and Heidelberg, 1991.

[2] T. M. Jovin, K. Rippe, N. B. Ramsing, R. Klement, W. Elhorst, and M. Vojtíškŏvá, *in* "Structure and Methods, Volume 3: DNA and RNA" (R. H. Sarma and M. H. Sarma, eds.), p. 155. Adenine Press, Schenectady, New York, 1990.

ps-DNA, originally proposed in a theoretical study by Pattabiraman,[3] are the trans-Crick–Watson (reverse Watson–Crick) base pairing with the glycosidic bonds in a trans orientation[4–6] and the lack of distinct major and minor grooves.[2,4,7] The ps helix is right-handed with a helical twist comparable to that of B-DNA, as determined from studies of a ps insert incorporated into a plasmid vector.[8] Parallel-stranded duplexes exhibit spectroscopic, thermodynamic, and biochemical properties different from those of conventional antiparallel B-DNA, and they are remarkably stable.[1,2,9] In the following we present the methods currently available for the synthesis and characterization of ps-DNA.

## Design of Oligonucleotides

### *Strategies for Constructing Parallel-Stranded Duplexes*

The stability of the ps duplexes examined to date decreases in the order homopolymeric d(A)·d(T) sequences,[4,5,9,10] mixed homopolymeric and alternating d(A·T) sequences,[7,9,11–13] and strictly alternating d(A-T) sequences.[10,14] Interspersed d(G·C) base pairs can be incorporated in mixed d(A·T) sequences but destabilize the ps duplex.[13,15] Other base pairing schemes in a trans orientation with at least two hydrogen bonds have been analyzed theoretically[16] and are under current investigation; they are not treated here.

[3] N. Pattabiraman, *Biopolymers* **25,** 1603 (1986).
[4] J. H. van de Sande, N. B. Ramsing, M. W. Germann, W. Elhorst, B. W. Kalisch, E. von Kitzing, R. T. Pon, R. M. Clegg, and T. M. Jovin, *Science* **241,** 551 (1988).
[5] M. W. Germann, H. J. Vogel, R. T. Pon, and J. M. van de Sande, *Biochemistry* **28,** 6220 (1989).
[6] C. Otto, G. A. Thomas, K. Rippe, T. M. Jovin, and W. L. Peticolas, *Biochemistry* **30,** 3062 (1991).
[7] N. B. Ramsing and T. M. Jovin, *Nucleic Acids Res.* **16,** 6659 (1988).
[8] J. Klysik, K. Rippe, and T. M. Jovin, *Nucleic Acids Res.* **19,** 7145 (1991).
[9] N. B. Ramsing, K. Rippe, and T. M. Jovin, *Biochemistry* **28,** 9528 (1989).
[10] O. F. Borisova, Y. B. Golova, B. P. Gottikh, A. S. Zibrov, I. A. Il'ychova, Y. P. Lysov, O. K. Mamayeva, B. K. Chernov, A. A. Chernyi, A. K. Shchyolkina, and V. L. Florentiev, *Mol. Biol. (U.S.S.R.)* **23,** 1535 (1989).
[11] M. W. Germann, B. W. Kalish, and J. M. van de Sande, *Biochemistry* **27,** 8302 (1988).
[12] K. Rippe, N. B. Ramsing, and T. M. Jovin, *Biochemistry* **28,** 9536 (1989).
[13] D. Rentzeperis, K. Rippe, T. M. Jovin, and L. A. Marky, *J. Am. Chem. Soc.*, in press.
[14] M. W. Germann, B. W. Kalish, R. T. Pon, and J. H. van de Sande, *Biochemistry* **29,** 9426 (1990).
[15] K. Rippe, N. B. Ramsing, R. Klement, and T. M. Jovin, *J. Biomol. Struct. Dyn.* **7,** 1199 (1990).
[16] I. A. Il'Ychova, Y. P. Lysov, A. A. Chernyi, A. K. Shchyolkina, B. P. Gottikh, and V. L. Florentiev, *J. Biomol. Struct. Dyn.* **7,** 879 (1990).

With mixed d(A·T) sequences, the parallel-stranded helix conformation is 20–30% less stable (in terms of the transition enthalpy) than an equivalent antiparallel-stranded (aps) molecule (Table I). Thus, it is necessary to restrict the degree to which alternative double helical configurations can arise within a designed sequence. Examples of different strategies for achieving this are shown in Fig. 1. The first experimental demonstration of ps-DNA[4] was with a set of hairpins having a $d(A)_{10}\cdot d(T)_{10}$ stem and $d(G)_4$ or $d(C)_4$ loops, as shown in Fig. 1A (ps-C10). These hairpins had a 5′–p–5′ or 3′–p–3′ linkage in the loop such that the strands in the stem were forced into a parallel orientation. Other homopolymeric d(A)·d(T) ps hairpins with a stem length of 8, 10,[5,9] or 15 base pairs (bp) (Table II,

TABLE I
THERMODYNAMIC PARAMETERS FOR PS AND APS HELIX INITIATION AND HELIX GROWTH[a]

| Parameter | ps-DNA (kJ mol$^{-1}$) | aps-DNA (kJ mol$^{-1}$) |
|---|---|---|
| $\Delta H_\beta$ (hairpins) | 25 | 25 |
| $\Delta H_\beta$ (linears) | 44 | 44 |
| $\Delta H_s$ (AA/TT) | −24 | −29 |
| $\Delta H_s$ (AT/TA) | −18[b] | −36[c] |
| $\Delta H_s$ (TA/AT) | — | −23[c] |
| | (kJ mol$^{-1}$ K$^{-1}$) | (kJ mol$^{-1}$ K$^{-1}$) |
| $\Delta S_\beta$ (hairpins) | 0.053 | 0.053 |
| $\Delta S_\beta$ (linears) | 0.152 | 0.152 |
| $\Delta S_s$ (AA/TT) | −0.072 | −0.084 |
| $\Delta S_s$ (AT/TA) | −0.058 | −0.096[c] |
| $\Delta S_s$ (TA/AT) | — | −0.084[c] |

[a] The values for helix initiation are indexed with a $\beta$ and those for helix elongation with an S. The nearest-neighbor interactions (in the 5′ → 3′ direction) as well as the initiation contribution were derived from a least-squares fit of the experimentally determined $\Delta H_{vH}$ and $\Delta S$ values given in Table II. It was assumed that the enthalpy and entropy transition terms are a linear combination of the nearest-neighbor values corresponding to the oligonucleotide sequence. The initiation contribution for hairpins and linear duplexes was set to be the same for the parallel and antiparallel stranded molecules in the fit. The data refer to helix growth rather than dissociation.

[b] Note that in ps-DNA AT/TA and TA/AT are equivalent because of symmetry.

[c] The aps AT/TA and TA/AT enthalpy and entropy interactions could not be determined accurately because all sequences had only a difference of one in the number of AT/TA and AT/TA nearest-neighbor interactions and the equation system for the aps molecules has an extra variable. See K. J. Breslauer, R. Frank, H. Blöcker, and L. A. Marky, *Proc. Natl. Acad. Sci. U.S.A.* **83,** 3746 (1986), for other values.

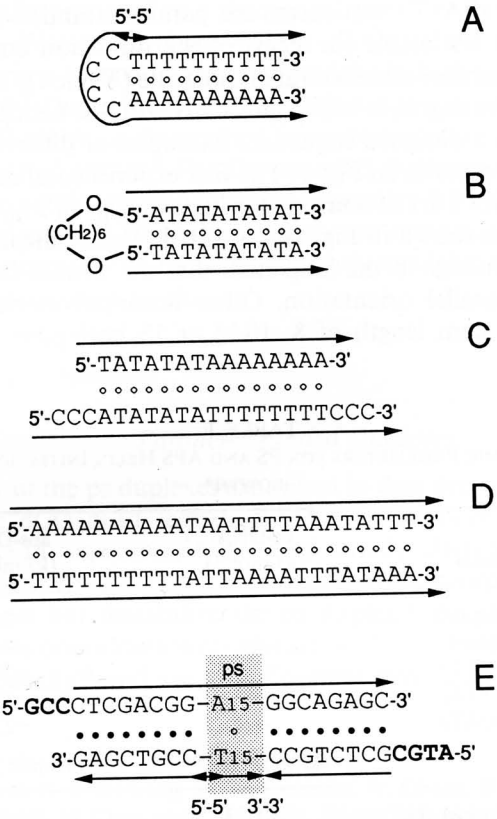


FIG. 1. Different strategies for obtaining parallel-stranded DNA. The trans-Crick–Watson base pairs (reverse Watson–Crick) of the parallel-stranded duplex are shown by the symbol (◦). (A) Hairpin structure designated as ps-C10 with a 5′–p–5′ linkage in the loop and 10 d(A·T) base pairs in the stem.[4,5,9] (B) Hairpins formed by chemical cross-linking of two DNA strands with a hexanediol bridge.[10,17] (C) Duplexes formed with strands of unequal length so as to constrain hybridization in the parallel orientation.[11] (D) Duplexes formed by hybridization of sequences with perfect complementarity only in the parallel orientation. The 25-nt duplex ps-D1·D2 is shown.[12] D1 is the upper strand, and D2 is the bottom strand. (E) Duplexes consisting of aps–ps–aps segments and terminal overlaps for insertion into a vector and circularization.[8] The bottom strand, designated as P5, contains 3′–p–3′ and 5′–p–5′ linkages that lead to inversion of polarity of the central 15 dT residues. The conventional cis-Watson–Crick base pairs of the antiparallel flanking regions are shown by the symbol (•).

ps-C15) and alternating d(A-T) hairpins with a stem of 8 or 10 bp[14] have been characterized. The introduction of 5′–p–5′ and 3′–p–3′ phosphodiester bonds can also be used to construct duplexes that have a ps insert with aps flanking regions (Fig. 1E, ps-P3·P5).[8] With appropriate overhangs such a duplex can be ligated into suitable plasmid vectors according to protocols described by Klysik *et al.*[8] in order to study the influence of topological stress on the insert.

An alternative for synthesizing ps-DNA hairpins is to chemically cross-link the ends of two DNA strands. This can be accomplished by introducing a 1,6-hexanediol linker[10,17] (Fig. 1B) or with bifunctional cross-linking reagents (M. Vojtíškŏvá and T. Jovin, unpublished) acting on 5′-terminal amino or sulfhydryl groups. Cross-linking via the 1,6-hexanediol linker has been reported for alternating d(A-T) sequences,[10,17] homopolymeric d(A)·d(T) sequences,[10,17] and mixed sequences also containing d(G·C) base pairs.[18]

It is not necessary to use the chemical modifications of the primary DNA structure mentioned above if the sequence is chosen such that complementarity in the parallel direction is more favorable than that in the case of alternative antiparallel secondary structures. Examples of appropriate sequences are given in Fig. 1C,D. With the ps construct in Fig. 1C the overhanging dC residues in the bottom strand are necessary to prevent the formation of antiparallel concatamers.[11] In the ps linear duplex ps-D1·D2 (Fig. 1D) the strands are fully base paired, and potential aps secondary structures are suppressed by the selected sequence.[12] A strategy of computer-aided search for such a sequence through all possible combinations of dA and dT in a segment of a given length is outlined in the next section.

### *Evaluation of Sequences for Parallel-Stranded Linear Duplexes*

The formation of alternative aps double helical configurations in selected sequences can be minimized with a computer program. The following input parameters are required: (i) length $n$ of the desired sequence: (ii) maximal number of base pair interactions $m_{hom}$ tolerated in aps homodimeric complexes, that is, through self-pairing of two copies of the given sequence such that the strands can adopt any staggered relative position; (iii) maximal number of base pair interactions $m_{het}$ tolerated in aps heterodimer complexes between the given sequence and its inverted complement

[17] A. K. Shchyolkina, Y. P. Lysov, I. A. Il'Ychova, A. A. Chernyi, Y. B. Golova, and B. K. Chernov, B. P. Gottikh, and V. L. Florentiev, *FEBS Lett.* **244,** 39 (1989).

[18] N. A. Tchurikov, B. K. Chernov, Y. B. Golova, and Y. D. Nechipurenko, *FEBS Lett.* **257,** 415 (1989).

(i.e., the complementary strand constituting the idealized fully paired ps duplex).

We evaluate sequences consisting only of A and T and represent them as a binary number, assigning the values 0 and 1 to T and A, respectively. Consider, for example, the 25-nucleotide (nt) sequence D1 (Fig. 1D). We test for condition (ii) above by using two D1 strands aligned in all possible aps orientations (without bulges) and score for the maximal number of aps A·T base pairs (14) and the longest run without mismatches (8). If this number is less than or equal to $m_{\text{hom}}$, the program performs the same test for condition (iii) using the D1 + D2 combination and the parameter $m_{\text{het}}$. In our example, a maximum of 12 bp can form, and the longest run of base pairs is 10 (Fig. 2). In general, upon specifying the length $n$, all possible sequences (of which $2^{n-1}$ are nonredundant) are examined and ranked in a hierarchy of desirability based on the lowest number of the possible aps homodimeric and heterodimeric interactions, including those that can

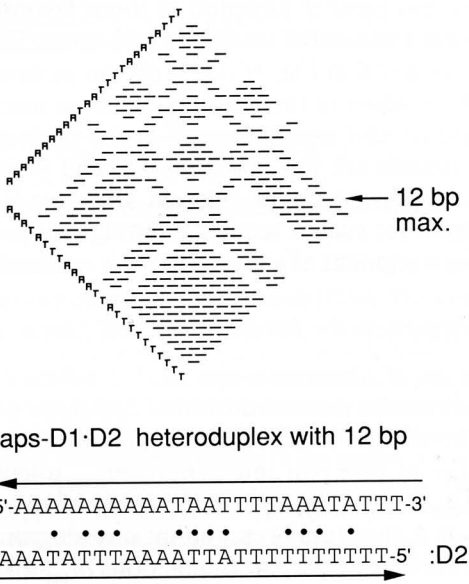


FIG. 2. Matrix plot for graphic display of competitive aps secondary structures. The antiparallel secondary structures (aps heteroduplexes) that can be formed from strands D1 and D2 (Fig. 1D are shown). The positions of potential base pairing are given by lines. All possibilities arising from pairing of the two strands in an antiparallel orientation are displayed. The combination with the maximum number of base pairs (12) is indicated by an arrow and is reproduced at the bottom. In the same way D1 can be plotted against D1 to evaluate potential aps homoduplexes.

arise in intermolecular interactions, also considering overhangs. Such an approach yields a family of sequences which then can be displayed graphically (Fig. 2) for studying the localization of the base-paired parts within the sequence. In our experience, the best ps versus aps discrimination is provided by sequences consisting of a homopolymeric segment ($\sim 0.4n$ in length) juxtaposed to a mixed A,T stretch, such that the maximal number of potential aps interactions is limited to about $n/2$.

The general strategy has been to generate an oligonucleotide quartet consisting of the selected sequence [e.g., D1], its ps complement [D2], and the two respective inverses [D4 and D3], such that two pairs of ps and aps duplexes can be formed, [ps-D1 · D2 and ps-D3 · D4] and [aps-D1 · D3 and aps-D2 · D4].[12] These can be studied and compared by numerous analytical techniques in order to elucidate the significant features common to or distinctive between the two conformations. The sequence repertoire can be extended by introduction of interesting substitutions, for example, the replacement of d(A · T) by d(G · C) base pairs.[15]

## Prediction of Thermodynamic Parameters from Sequence

### *Concept of Nearest-Neighbor Approximation*

Given the sequence of a potential ps duplex structure one can estimate its stability. The standard enthalpy $\Delta H^\circ$ and the entropy $\Delta S^\circ$ differences for the coil–helix transition are determined mainly by the stacking interactions of two adjacent bases, that is, the nearest-neighbors. Thus it is possible to decompose a duplex into its different nearest-neighbor quartets and derive $\Delta H^\circ$ and $\Delta S^\circ$ by adding the contributions of nearest-neighbors and an additional nucleation term[19–21] according to Eqs. (1) and (2).[22] Next-nearest-neighbor interactions are not considered. The indices $\beta$ and s refer to helix initiation and elongation, respectively. The total number of base pairs formed is $n$.

$$\Delta H^\circ = \Delta H_\beta^\circ + \sum_{i=1}^{n-1} \Delta H_{s_i}^\circ \qquad (1)$$

[19] K. J. Breslauer, R. Frank, H. Blöcker, and L. A. Marky, *Proc. Natl. Acad. Sci. U.S.A.* **83,** 3746 (1986).

[20] S. Freier, R. Kierzek, J. A. Jaeger, N. Sugimoto, M. H. Caruthers, T. Neilson, and D. H. Turner, *Proc. Natl. Acad. Sci. U.S.A.* **83,** 9373 (1986).

[21] O. C. Uhlenbeck, P. N. Borer, B. Dengler, and I. Tinoco, Jr., *J. Mol. Biol.* **73,** 483 (1973).

[22] In the expression for the entropy change an additional term $\Delta S_{sym}$ has to be included for self-complementary DNA according to Breslauer *et al.*[19]

$$\Delta S^\circ = \Delta S_\beta^\circ + \sum_{i=1}^{n-1} \Delta S_{s_i}^\circ \qquad (2)$$

Based on Eqs. (1) and (2), a least-squares algorithm was applied to the measured data presented in Table II in order to determine the best global estimate for the different nearest-neighbor interactions and initiation parameters for the coil–helix transition of ps hairpins and ps linear duplexes. The resultant values are presented in Table I and were used to calculate the thermodynamic quantities given in Table II in the form of a comparison with the measured values. The agreement is generally satisfactory.

In the following we use the designation $\Delta H_{vH}$ (van't Hoff enthalpy of melting) instead of $\Delta H^\circ$ to indicate that the analyzed values were primarily determined from thermal transitions using optical measurements and not calorimetrically. The parameters in Eqs. (3)–(6) and in Table II are given for the helix–coil transition rather than for the inverse process referred to in Eqs. (1) and (2) and in Table I. The entropy change $\Delta S$ was referenced to 0.1 *M* NaCl by using the melting point $T_m$ in 0.1 *M* NaCl and a total strand concentration $C_t$ of 2 $\mu M$ for the linear duplexes. The melting enthalpy $\Delta H_{vH}$ was assumed to be salt independent in the range from 0.1 to 1.0 *M* NaCl.[9,12]

*Procedure: Estimation of $\Delta H_{vH}$, $\Delta S$, and $T_m$ for Helix–Coil Transition of a Given Parallel-Stranded Hairpin or Linear Duplex and Its Antiparallel-Stranded Reference*

*Estimation of $\Delta H_{vH}$ and $\Delta S$.* The number of AA/TT ($n_{AA}$) and AT/TA ($n_{AT}$) nearest-neighbors [and in the case of the aps reference molecules the number of TA/AT ($n_{TA}$) as well] are counted for the given sequence. In the ps-D1·D2 duplex, for example, $n_{AA} = 17$ and $n_{AT} = 7$. Note that in ps-DNA there is no distinction between AT/TA and TA/AT nearest neighbors, since the strand backbone orientation is identical. Then, $\Delta H_{vH}$ and $\Delta S$ are calculated according to the following equations:

Parallel-stranded hairpin (linear) transition

$$\Delta H_{vH} = [-25(-44) + 23.6n_{AA} + 18.3n_{AT}] \quad \text{kJ mol}^{-1} \qquad (3)$$

$$\Delta S = [-0.05(-0.15) + 0.072n_{AA} + 0.058n_{AT}] \quad \text{kJ mol}^{-1} \qquad (4)$$

Antiparallel-stranded hairpin (linear) transition

$$\Delta H_{vH} = [-25(-44) + 28.7n_{AA} + 35.5n_{AT} + 22.6n_{TA}] \quad \text{kJ mol}^{-1} \qquad (5)$$

$$\Delta S = [-0.05(-0.15) + 0.084n_{AA} + 0.096n_{AT} + 0.084n_{TA}] \quad \text{kJ mol}^{-1}\,\text{K}^{-1} \qquad (6)$$

TABLE II
THERMODYNAMIC DATA FOR HELIX–COIL TRANSITIONS OF PS-DNA AND APS-DNA[a]

| DNA duplex | $\Delta H_{vH}$[b] (kJ mol$^{-1}$) | | $\Delta S$[c] (kJ mol$^{-1}$ K$^{-1}$) | | $T_m$[d] (°C) | |
|---|---|---|---|---|---|---|
| | Exp. | Calc. | Exp. | Calc. | Exp. | Calc. |
| ps-C8[e] | 153 | 140 | 0.50 | 0.45 | 35 | 38 |
| ps-C10[e] | 202 | 188 | 0.64 | 0.60 | 40 | 42 |
| ps-C15[f] | 250 | 306 | 0.79 | 0.96 | 43 | 47 |
| ps-C8_alt[g] | 106 | 103 | 0.36 | 0.35 | 19 | 19 |
| ps-C10_alt[g] | 137 | 140 | 0.47 | 0.47 | 21 | 25 |
| ps-F5·F6[h] | 235 | 249 | 0.72 | 0.76 | 8 | 10 |
| ps-15-mer[i] | 309 | 246 | 0.97 | 0.76 | 11 | 10 |
| ps-C2·C3[j] | 353 | 401 | 1.06 | 1.22 | 25 | 26 |
| ps-D1·D2[k] | 500 | 485 | 1.40 | 1.48 | 31 | 30 |
| ps-D3·D4[j] | 507 | 485 | 1.56 | 1.48 | 29 | 30 |
| aps-C8[e] | 184 | 176 | 0.58 | 0.56 | 45 | 38 |
| aps-C10[e] | 230 | 234 | 0.71 | 0.73 | 51 | 45 |
| aps-C15[f] | 362 | 377 | 1.10 | 1.15 | 57 | 52 |
| aps-C10_alt[g] | 244 | 243 | 0.78 | 0.76 | 39 | 47 |
| aps-F5·F7[h] | 352 | 354 | 1.11 | 1.06 | 27 | 26 |
| aps-15-mer[i] | 487 | 366 | 1.47 | 1.07 | 33 | 34 |
| aps-C3·C7[j] | 546 | 523 | 1.62 | 1.55 | 40 | 39 |
| aps-D1·D3[k] | 654 | 653 | 1.92 | 1.92 | 49 | 48 |
| aps-D2·D4[j] | 628 | 641 | 1.86 | 1.91 | 44 | 43 |

[a] The listed parameters were obtained from experiments with 0.1–1.0 *M* NaCl and 10 m*M* sodium cacodylate, pH 7.2. The calculated values (Calc.) were determined according to the Eqs. (3)–(6) given in the text.

[b] $\Delta H_{vH}$ is the average van't Hoff enthalpy of melting. No correlation with salt concentration in the range 0.1–1.0 *M* NaCl was found.[9,12] The $\Delta H_{vH}$ values are within ±10% experimental error as estimated from completely independent experiments.

[c] The entropy was calculated by using the average $\Delta H_{vH}$ and the $T_m$ in 0.1 *M* NaCl calculated from linear regressions in 0.05–0.8 *M* NaCl.

[d] $T_m$ in 0.1 *M* NaCl (including the buffer contribution of 0.11 *M* NaCl) and scaled for the linear duplexes to a strand concentration of 2.0 $\mu M$ according to Eq. (8). The $T_m$ values are within ±4° experimental error as estimated from completely independent experiments.

[e] Average values from Ramsing *et al.*[9] and Germann *et al.*[5]

[f] K. Rippe, Ph.D. Thesis, University of Göttingen, 1991. The molecule ps-C15 is a hairpin with 15 homopolymeric d(A·T) base pairs in the stem and a $C_4$ loop.

[g] Germann *et al.*[14] The $T_m$ in 0.1 *M* NaCl was estimated from given values in 0.8 *M* NaCl using the salt dependence of $T_m$ determined in Ramsing *et al.*[9]

[h] K. Rippe, Ph.D. Thesis, University of Göttingen, 1991. The duplexes ps-F5·F6 and aps-F5·F7 have the same sequence as ps-F1·F2 and aps-F1·F4, respectively[2] but no 5′-terminal amino group.

[i] Germann *et al.*,[11] not included in the least squares fit because of single-stranded regions present at the ends of the duplex (Fig. 1C).

[j] Ramsing *et al.*[9]

[k] Average values from Rippe *et al.*[12] and Rentzeperis *et al.*[13]

The initiation contribution is different for hairpins and linear duplexes. In Eqs. (3)–(6) the values for the initiation of the linear duplexes are given in parentheses. It is possible to incorporate d(G·C) base pairs into a parallel-stranded duplex, but they destabilize the structure.[15] The database is yet too small to derive $\Delta H_s$ and $\Delta S_s$ values of the different AG/TC, GA/CT, and GT/CA nearest-neighbor interactions in ps-DNA. However, based on available data[13,15] we have estimated an average contribution of $-14$ kJ mol$^{-1}$ for $\Delta H_s$ and $-0.05$ kJ mol$^{-1}$ K$^{-1}$ for $\Delta S_s$.

*Estimation of melting point $T_m$ from $\Delta H_{vH}$ and $\Delta S$.* The melting point $T_m$, the midpoint of the helix–coil transition, can be calculated according to a two-state model from Eqs. (7) and (8)[9]:

Hairpin transition:
$$T_m = \frac{\Delta H_{vH}}{\Delta S} \tag{7}$$

Linear duplex transition:
$$T_m = \frac{\Delta H_{vH}}{\Delta S - R \ln(C_t/4)} \tag{8}$$

where $R$ is the gas constant (8.314 J mol$^{-1}$ K$^{-1}$) and $C_t$ the total strand concentration in M units. As evident from Eqs. (7) and (8), $T_m$ of the hairpins is independent of concentration, whereas $T_m$ of the linear duplexes depends on $C_t$. The derived values of $T_m$ in Table II correspond to $C_t = 2 \times 10^{-6}\ M$ for the linear duplexes. At this concentration $R \ln(C_t/4) = -0.121$ kJ mol$^{-1}$ K$^{-1}$.

If the concentration of the two strands is not equimolar, as, for example, in experiments in which only on strand is $^{32}$P-labeled and the complementary unlabeled strand with the concentration $C_i$ is in great excess, $T_m$ can be estimated according to the expression

$$\frac{1}{T_m} = \frac{1}{T_{mref}} - \frac{R}{\Delta H_{vH}} \ln\left(\frac{4C_i}{C_t}\right) \tag{9}$$

In Eq. (9) $T_{mref}$ is the reference $T_m$ of an equimolar mixture of strands with a total strand concentration $C_t$ under the same salt conditions.[23]

*Effects of Salt on Thermodynamic Stability.* The $T_m$ values calculated according to Eqs. (3)–(8) correspond to the reference condition of 0.1 $M$ NaCl. At other salt concentrations, $T_m$ can be derived from the slope of the $T_m$ versus log[Na] curve. The salt dependence, namely, the change of $T_m$ per decade of salt concentration $\Delta T_m/\Delta$ log[Na], is on average $17 \pm 2°$ for the ps and $16 \pm 1°$ for the aps references.[9] Thus a change in salt concentration from 0.05 to 0.5 $M$ increases the $T_m$ of a ps duplex by approximately 17°. $Mg^{2+}$ also exerts a stabilizing effect on both the ps and aps

[23] J. Klysik, K. Rippe, and T. M. Jovin, *Biochemistry* **29**, 9831 (1990).

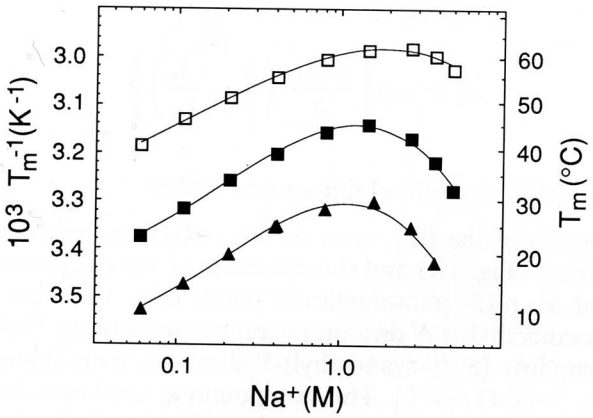


FIG. 3. Melting temperature of ps and aps linear duplexes as a function of salt concentration. Displayed are the duplexes ps-D1·D2 (■) (Fig. 1D); ps-D5·D6 (▲), a variant of ps-D1·D2 in which four d(A·T) base pairs are replaced by d(G·C) base pairs[15] and aps-D1·D3 (□), the aps reference for ps-D1·D2. The solid lines are a third order regression. The $T_m$ values were corrected to a total concentration of 1.6 $\mu M$ strands according to Eq. (8). The $Na^+$ concentration includes the contribution of the buffer.

duplexes, with the $T_m$ in 2 m$M$ $MgCl_2$ being equal to that in 0.2–0.3 $M$ NaCl.

The linear dependence of $T_m$ (or $1/T_m$) on log[$Na^+$] is only valid for $Na^+$ concentrations below 0.8 $M$. Above this value, $T_m$ passes through a maximum and then decreases with a further increase of [$Na^+$] (Fig. 3). This effect is known for B-DNA[24] but is more pronounced with the ps linear duplexes (Fig. 3). Measurements of absorption hyperchromicity and chemical reactivity with osmium tetroxide–pyridine (Os,py) show that high salt concentrations reduce the thermodynamic stability of the ps helix.[23] For example, the $T_m$ of ps-D1·D2 in 1.6 $M$ NaCl is 46° but decreases to 32° in 4.9 $M$ NaCl (Fig. 3). In addition, the helix–coil transition is less cooperative; $\Delta H_{vH}$ decreases by about 30%. Thus the fractional transition to the single-stranded state ($\theta$) calculated for a two-state model according to Eqs. (10) and (11)[9] can increase considerably at salt concentrations in the molar range:

Hairpin transition:
$$\theta = \frac{1}{1+E} \tag{10}$$

Linear duplex transition:
$$\theta = \frac{(1+8E)^{1/2}-1}{4E} \tag{11}$$

[24] C. F. Anderson and M. T. Record, Jr., *Annu. Rev. Phys. Chem.* **33,** 191 (1982).

with

$$E \equiv \exp\left[\frac{\Delta H_{vH}}{R}\left(\frac{1}{T} - \frac{1}{T_m}\right)\right]$$

## Synthesis and Purification of Oligonucleotides

The synthesis of the $dT_{10}$ tract in the ps-C10 hairpin molecule with 5′–p–5′ linkage (Fig. 1A) and the synthesis of the $dT_{15}$ tract within the 3′–p–3′ and 5′–p–5′ phosphodiester bonds (Fig. 1E) were carried out with 5′-(β-cyanoethyl-*N,N*-diisopropylamino)phosphinyl-3′-(4,4′-dimethoxytrityl)thymidine [5′-(β-cyanoethyl)-3′-dimethoxytritylthymidine phosphoramidite, 3′-DMTr-βdT]. This compound is synthesized as described below. In contrast to the procedure outlined by van de Sande *et al.*,[4] it is advantageous to use *tert*-butyldiphenylchlorosilane instead of *tert*-butyldimethylchlorosilane for the protection of the 5′-OH group of thymidine because of its higher specificity for the 5′-OH group. $N^6$-Benzoyl-5′-(β-cyanoethyl)-3′-dimethoxytrityladenosine phosphoramidite (3′-DMTr-$\beta dA^{bz}$) can be synthesized in a similar way by using commercially available $N^6$-benzoyl-2′-deoxyadenosine instead of thymidine as the starting material[12] or by introducing an extra step for the protection of the N-6 exocyclic amino group of adenine. Starting the synthesis in the 5′ → 3′ direction requires loading of the solid controlled-pore glass (CPG) support with the 3′-DMTr protected nucleoside. This can be done according to procedures used for the 5′-DMTr protected nucleoside.[25]

*Procedure: Synthesis of 5′-(β-Cyanoethyl-N,N-diisopropylamino)-phosphinyl-3′-(4,4′-dimethoxytrityl)thymidine*

*Protection of 5′-Hydroxyl Group of Thymidine with tert-Butyldiphenylchlorosilane.* Dissolve 5.0 g (20.7 mmol) thymidine in 100 ml dry pyridine and evaporate to remove traces of water. Then redissolve in 100 ml fresh pyridine. Add 2.9 ml (3.1 g, 11.4 mmol, 0.55 Eq) *tert*-butyldiphenylchlorosilane and after 30 min add another 2.9 ml *tert*-butyldiphenylchlorosilane. Monitor the reaction by thin-layer chromatography (TLC) with 9:1 (v/v) dichloromethane–methanol on a silica gel 60 plate with a fluorescent UV indicator 254 nm. The product 5′-(*tert*-butyldiphenyl)thymidine is depicted in Fig. 4A.

[25] M. J. Damha, P. A. Giannaris, and S. V. Zabarylo, *Nucleic Acids Res.* **18,** 3813 (1990). A detailed description of the synthesis of 3′-DMTr-$\beta dA^{bz}$ and the loading of the CPG support with 3′-DMTr thymidine and $N^6$-benzoyl-3′-DMTr adenosine will be published elsewhere (Wodarski *et al.*, in preparation).

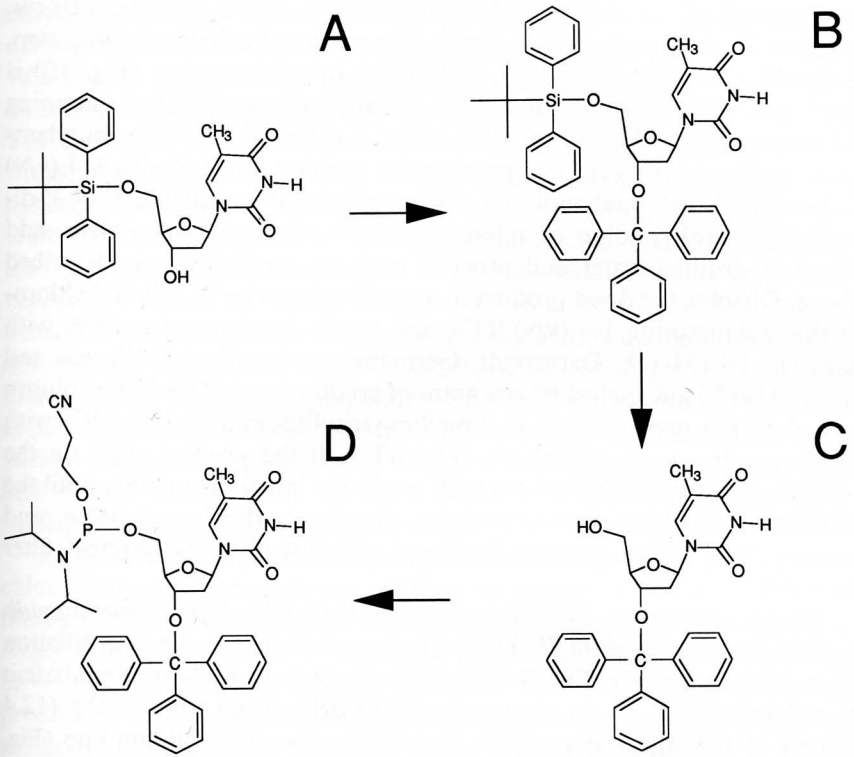


FIG. 4. Synthesis of 5′-(β-cyanoethyl-*N,N*-diisopropylamino)phosphinyl-3′-dimethoxytritylthymidine (3′-DMTr-βdT). (A) 5′-(*tert*-Butyldiphenyl)thymidine. (B) 5′-(*tert*-Butyldiphenylsilyl)-3′-(4,4′-dimethoxytrityl)thymidine. (C) 3′-(4,4′-Dimethoxytrityl)thymidine. (D) 5′-(β-Cyanoethyl-*N,N*-diisopropylamino)phosphinyl-3′-(4,4′-dimethoxytrityl)thymidine.

*Protection of 3′-Hydroxyl Group with 4,4′-Dimethoxytrityl Chloride.* Add 8.4 g (24.8 mmol, 1.2 Eq) 4,4′-dimethoxytrityl chloride (DMTr-Cl) to convert the 5′-(*tert*-butyldiphenylsilyl)thymidine (Fig. 4A) to 5′-(*tert*-butyldiphenylsilyl)-3′-(4,4′-dimethoxytrityl)thymidine (Fig. 4B). Monitor the reaction by TLC with 9 : 1 (v/v) dichloromethane–methanol and add more DMTr-Cl after 2 hr if necessary. If the reaction is complete, add 50 ml of distilled water, incubate for 10 min, evaporate to dryness, and dissolve in 250 ml ethyl acetate with 0.4% (v/v) triethylamine (TEA). The TEA is included here and in the following steps to prevent acid-catalyzed cleavage of the DMTr group. Extract the ethyl acetate phase first with 10% (w/v) aqueous $NaHCO_3$ and then with saturated aqueous NaCl. Dry the organic phase over $Na_2SO_4$, filter, evaporate, and reevaporate after addition of toluene.

*Removal of 5′-tert-Butyldiphenylsilyl Group with 1 M Tetrabutylammonium Fluoride in Tetrahydrofuran.* The product from the previous step, 5′-(*tert*-butyldiphenylsilyl)-3′-(4,4′-dimethoxytrityl)thymidine (Fig. 4B) is dried and then dissolved in 100 ml tetrahydrofuran (THF) containing 0.4% (v/v) TEA. Add 22.7 ml (20.7 mmol, 1.0 Eq) of 1.1 *M* tetrabutylammonium fluoride in THF and monitor the reaction by TLC with 9 : 1 (v/v) dichloromethane–methanol and with commercially available 5′-(4,4′-dimethoxytrityl)thymidine as reference. If the reaction is complete, add 50 ml of distilled water and proceed with the purification as described above. Dissolve the dried product in a small volume (~ 10 ml) of dichloromethane containing 1% (v/v) TEA and purify by chromatography with Kieselgel 60 (Merck, Darmstadt, Germany) as described by Sproat and Gait.[26] Use 20 g Kieselgel 60 per gram of crude material. Pack the column and elute the product 3′-(4,4′-dimethoxytrityl)thymidine (Fig. 4C) with dichloromethane containing 1% (v/v) TEA. If the product stays on the column, supplement the solvent with methanol in 1% increments until the product elutes. Evaporate to dryness, dissolve in dichloromethane, and precipitate by addition to rapidly stirred *n*-hexane (20–25 volumes); filter the solid.

*Phosphitylation of 5′-Hydroxyl Group with Chloro(β-cyanoethoxy)diisopropylaminophosphine.*[27] Dry diisopropylethylamine by distillation from calcium hydride. Distill dichloromethane from $P_2O_5$ and incubate it overnight with $Al_2O_3$ to remove traces of acid. Then weigh 3.0 g (12.4 mmol) of the silica gel-purified 3′-(4,4′-dimethoxytrityl)thymidine (Fig. 4C) in a dry 250-ml round-bottomed flask and coevaporate twice with dry dichloromethane containing 10% (v/v) dry pyridine. Add a magnetic stirrer, cap the flask with a rubber septum, insert an 18-gauge needle through the rubber septum, place the flask in a desiccator, and dry under reduced pressure overnight. Then break the vacuum in the desiccator by slowly introducing argon from a balloon into the desiccator. Open the desiccator and withdraw the venting needle. Inject a needle attached to an argon-filled balloon through the rubber septum of the round-bottomed flask as well as through the cap of the phosphitylating reagent chloro(β-cyanoethoxy)diisopropylaminophosphine.

In the following steps, all reagents are injected through the rubber septum with an oven-dried syringe. Start by injecting 8.6 ml diisopropyl-

[26] T. Sproat and M. J. Gait, *in* "Oligonucleotide Synthesis: A Practical Approach" (M. J. Gait, ed.), p. 199. IRL Press, Oxford, 1984.

[27] The procedure is similiar to the one described by T. Atkinson and M. Smith [*in* "Oligonucleotide Synthesis: A Practical Approach" (M. J. Gait, ed.), p. 35. IRL Press, Oxford, 1984], but a different phosphitylating reagent is used.

ethylamine (6.4 g, 49.6 mmol, 4 Eq) and then 30 ml dichloromethane, and dissolve the 3′-(4,4′-dimethoxytrityl)thymidine. Then add 4.2 ml (4.4 g, 18.6 mmol, 1.5 Eq) of the phosphitylating reagent chloro(β-cyanoethoxy) diisopropylaminophosphine. Stir the mixture and monitor the reaction by TLC in 45:45:10 (v/v) ethyl acetate–dichloromethane–triethylamine by withdrawing aliquots with a dry syringe. If the reaction is complete quench the excess phosphitylating reagent with 0.2 ml anhydrous methanol. Evaporate to dryness, dissolve in dichloromethane, and precipitate by addition to rapidly stirred *n*-hexane. Filter the solid, dissolve in a small volume (~10 ml) of 45:45:10 (v/v) ethyl acetate–dichloromethane–triethylamine, and purify by chromatography with Kieselgel 60 (Merck) as described by Sproat and Gait.[26] Use 20 g silica gel 60 per gram of crude material. Pack the column and elute the product with 45:45:10 (v/v) ethyl acetate–dichloromethane–triethylamine. Alternatively the column can be packed with *n*-hexane containing 0.4% (v/v) triethylamine and then equilibrated and eluted with 49:49:2 (v/v) *n*-hexane–dichloromethane–triethylamine, which is a less polar solvent that gives better resolution.

Evaporate the product-containing fractions to dryness, dissolve in dichloromethane, precipitate by addition to rapidly stirred *n*-hexane, and filter the solid. Then dry under reduced pressure in a desiccator over $P_2O_5$. Analyze the product by $^{31}P$ NMR in $CD_3CN$ from −10 to 190 ppm with 85% phosphoric acid as external standard. The two stereoisomers of the product 5′-(β-cyanoethyl-*N,N*-diisopropylamino)phosphinyl-3′-(4,4′-dimethoxytrityl)thymidine (Fig. 4D) appear around 150 ppm.

*Procedure: Automated Synthesis of 5′-p-5′ and 3′-p-3′ Phosphodiester Bonds with 3′-Dimethoxytrityl-Protected β-Cyanoethylthymidine*

Weigh the amount of 5′-(β-cyanoethyl)-3′-dimethoxytritylthymidine phosphoramidite (3′-DMTr-βdT) needed for the synthesis (usually 0.1–1.0 g) into a dark glass vial that can be attached to the synthesizer and cap it with a rubber septum. Insert an 18-gauge needle through the rubber septum, place the vial in a desiccator, and purge several times with argon. Then dry overnight under reduced pressure with the desiccator, connected to an oil pump. The next day slowly introduce argon from a balloon into the desiccator, open the desiccator, and withdraw the venting needle immediately. The 3′-DMTr-βdT is dissolved to give a concentration of 0.1 *M* in dry acetonitrile as for normal 5′-DMTr β-cyanoethyl-protected phosphoramidites. It is important to check the solubility of the 3′-DMTr-βdT phosphoramidite. If insoluble particles remain in the solution severe problems may arise during synthesis because of blocking of delivery lines.

Coupling in the 5′ → 3′ direction is about 4 times slower because of the

lower reactivity of the 3′-OH group.[28] To account for the difference, two modifications are introduced into the synthesis cycle. First, the 3′-DMTr-βdT + tetrazole delivery is increased by about 25% and the tetrazole delivery by about 20%. For the 1 μmol scale synthesis on an Applied Biosystems (Foster City, CA) synthesizer this is done by introducing an extra 3′-DMTr-βdT + tetrazole delivery step for 5 sec followed by an extra tetrazole delivery step for 3 sec. Then, an additional wait step of 2 min is introduced for the 3′-DMTr-βdT port. The efficiency of coupling can be monitored by spectrophotometrically measuring the liberated DMTr cation and is as high as with the 5′-DMTr β-cyanoethyl-protected phosphoramidites. Incorporation of the 5′–p–5′ and 3′–p–3′ phosphodiester bonds at the desired positions in the sequence is accomplished by switching from the conventional 5′-DMTr β-cyanoethyl-protected phosphoramidite to 3′-DMTr-βdT and vice versa during synthesis.

### *Oligonucleotide Purification*

Purification is according to standard protocols. We have no indication that the 5′–p–5′ or 3′–p–3′ phosphodiester bonds lead to unusual chromatographic behavior. We use the following procedure. After synthesis with a terminal DMTr group, the protecting groups liberated by treatment with concentrated ammonia are removed by a Sephadex G-25 column. After purification by reversed-phase chromatography and detritylation, anion-exchange chromatography on a fast-protein–high-performance liquid chromatography (FPLC/HPLC) system is carried out.[29] The last step consists of desalting on a Sephadex G-25 column.

## Characterization of Oligonucleotides and Parallel-Stranded Duplexes

### *Ultraviolet Absorbance Spectroscopy*

Several spectroscopic methods have been used for characterization of the ps conformation.[1,2] They include ultraviolet absorption,[2,4,7,11,12,14,15] circular dichroism,[4,5,7,11,12,15] Raman,[6] $^{31}$P NMR,[2,5] and $^{1}$H NMR[5] spectroscopy. In this chapter we restrict ourselves to measurements of UV absorption because it requires only simple instrumentation and gives characteristic differences for the ps and aps duplexes.

[28] B. Kaplan and K. Itakura, *in* "DNA Synthesis on Solid Supports and Automation" (S. A. Narang, ed.), p. 9. Academic Press, Orlando, Florida, 1987.

[29] For details on HPLC purification of synthetic DNA, see [2] in this volume.

*Extinction Coefficients.* The UV absorbance extinction coefficient for dA·dT oligonucleotides was determined by phosphate analysis of a 21-nucleotide sequence: 8.6 m$M$ (base)$^{-1}$ cm$^{-1}$ at 264 nm in the denatured state at 70°; buffer 0.1 $M$ NaCl, 10 m$M$ sodium cacodylate, pH 7.2.[7] The wavelength of 264 nm was chosen to compensate for the different ratios of dA and dT with other sequences, because it corresponds to an isosbestic point for poly[d(A)] and poly[d(T)] under approximately the same conditions.[30] We have also calculated an idealized value of 8.6 m$M$ (base)$^{-1}$ cm$^{-1}$ at 264 nm and 70° for a dG residue in a mixed sequence from the expression $2\varepsilon\{\text{poly[d(G-C)]}_{70°,264nm}\} - \varepsilon\{\text{poly[d(C)]}_{70°,264nm}\}$.[15] With the extinction coefficients in the denatured state at 70° of 8.6 m$M$ (base)$^{-1}$ cm$^{-1}$ for dA, dT, and dG residues and 7.3 m$M$ (base)$^{-1}$ cm$^{-1}$ for dC,[31] one can calculate the extinction coefficient of a given sequence, assuming additivity of unit contributions.

The linear ps-DNA duplexes are prepared by mixing equimolar amounts of the desired oligonucleotides in the specified salt solutions, heating to 70° for 5 min, and cooling slowly to room temperature. The heating step might not be necessary if the single strands cannot form stable secondary structures. Solutions of sodium cacodylate are used as buffers because they are antibacterial, as opposed to phosphate buffers, and their pH does not vary appreciably with temperature, as with Tris-HCl.

*Ultraviolet Spectra of Parallel-Stranded Duplexes and Their Antiparallel-Stranded References.* The UV spectra of the ps-D1·D2 (Fig. 1D) and aps-D1·D3 molecules are shown in Fig. 5 in different representations. The native ps-D1·D2 duplex shows a blue shift of the absorbance maximum relative to the aps-D1·D3 reference, whereas the spectra in the denatured state are nearly identical (Fig. 5A and 5B). The difference presumably reflects particular features of the electronic structure and stacking geometry of ps-DNA. A plot of the ratio of the absorbances in the denatured and native states versus wavelength emphasizes the characteristic differences between ps-DNA and aps-DNA in a manner independent of concentration (Fig. 5C). By choice of appropriate wavelength, absorbance ratios can be derived that demonstrate the qualitative differences in the spectra and melting temperature of ps- and aps-DNAs (Fig. 5D). Thus the $A_{250}/A_{284}$ ratio decreases in the case of ps-DNA but increases on denaturation of aps-DNA. Other spectral data, including that of DNAs with trans-d(G · C) base pairs, are given elsewhere.[2,15]

The thermally induced helix–coil transitions measured by UV absorption spectroscopy can be visualized by normalizing the absorbances at each

[30] M. Riley, B. Maling, and M. J. Chamberlin, *J. Mol. Biol.* **20,** 359 (1966).
[31] R. Inman, *J. Mol. Biol.* **9,** 624 (1964).

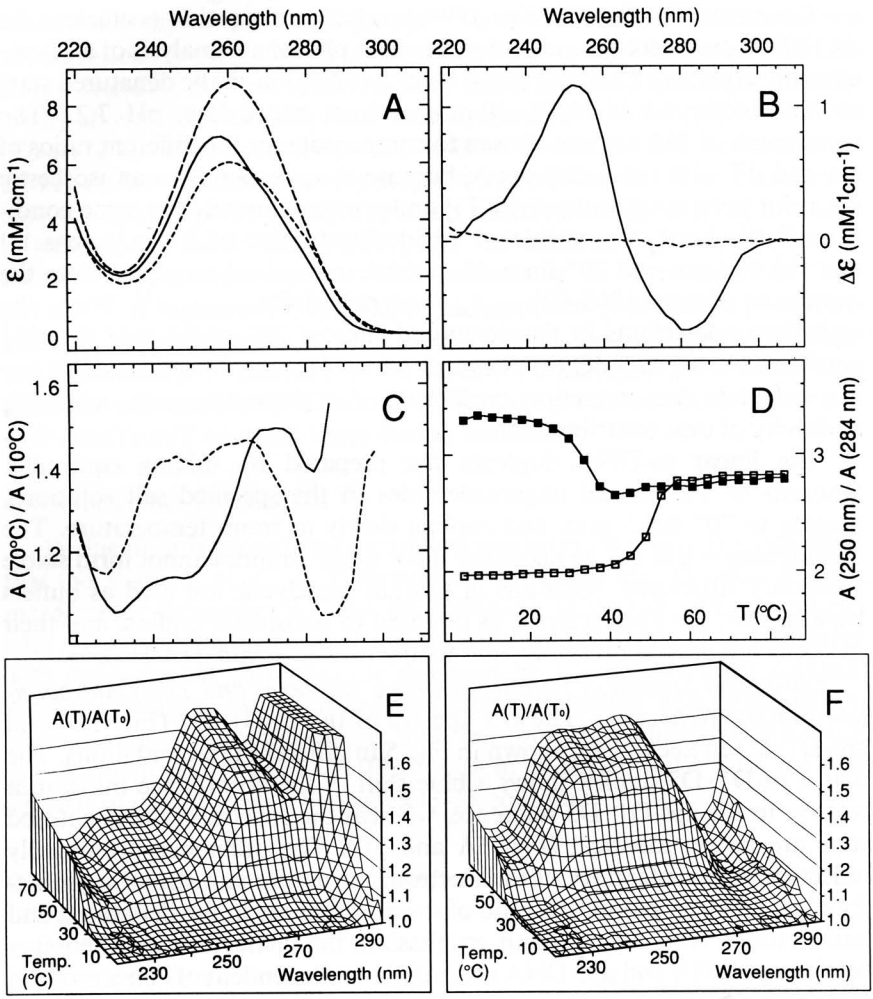


FIG. 5. Various ways to visualize the difference in UV absorption between ps- and aps-DNA. (A) UV spectra at 10° of ps-D1·D2 (—) and aps-D1·D3 (---); at 70° melted ps-D1·D2 duplex (– – –) and melted aps-D1·D3 duplex (····). (B) UV difference spectra (ps-D1·D2 − aps-D1·D3) at 10° (—) and at 70°(---). (C) Hyperchromicity spectra expressed as the ratio of absorbances at 70° and 10° of ps-D1·D2 (—) and aps-D1·D3 (---). (D) Wavelength-dependent melting curve of ps-D1·D2 (■) and aps-D1·D3 (□). The ratio of UV absorbances at 250 and 284 nm is plotted versus temperature. (E, F) Thermally resolved ultraviolet absorption spectra of ps and aps helices. The ratio $A_\lambda(T)/A_\lambda(T_0)$, where $T_0$ is the initial temperature, is plotted versus temperature for (E) ps-D1·D2 and (F) aps-D1·D3. Spectra (A)–(C) were recorded in 0.1 *M* NaCl, 10 m*M* sodium cacodylate, pH 7.2, and spectra (D)–(F) were measured in 2 m*M* $MgCl_2$ and 10 m*M* sodium cacodylate, pH 7.2. (Data in part are from Rippe *et al.*[12])

temperature $T$ and wavelength $\lambda$ to the values at the initial (low) temperature $T_0$. The resultant three-dimensional plots (Fig. 5E,F) reveal a characteristic pattern for both the ps and the aps conformation.[2,7,12,15] Whereas the ps duplexes show a peak around 270 nm and a strong increase of the absorbance ratio beginning at 280 nm, the aps reference molecules have a plateau from 240 to 270 nm and show little hyperchromicity from 280 to 290 nm.

*Native Gel Electrophoresis*

Gel electrophoresis under native conditions for ps and aps duplexes in the range of 15–40 base pairs can be carried out on a 14% polyacrylamide (acrylamide–bisacrylamide, 19:1) gel in 89 m*M* Tris–borate (pH ~ 8) and 2 m*M* $MgCl_2$ (TBM), that is, in the normally used TBE buffer but with EDTA replaced by 2 m*M* $MgCl_2$. As loading solutions 5× Ficoll loading buffer [containing 15% Ficoll (w/v), 0.3% bromphenol blue, and 0.3% xylene cyanole in TBM buffer] or 5× sucrose loading buffer [containing 40% sucrose (w/v), 0.3% bromphenol blue, and 0.3% xylene cyanole in TBM buffer] are appropriate. It is important to achieve an effective temperature control of the gel during electrophoresis in order to avoid denaturation of the duplexes being resolved. We use a system in which the gel is completely immersed in the lower buffer, which in turn is cooled by a water bath. The voltage applied should not exceed 10 V/cm. The gel shown in Fig. 6 was run under these conditions at 20°.

An important finding from the electrophoretic analysis is that the ps duplexes have slightly higher electrophoretic mobilities on gels than their aps references.[4,7,11,12] With the duplexes analyzed in Fig. 6 this difference is less evident because the ps-P3·P5 duplex (Fig. 1E) has aps flanking sequences.

*Drug Binding*

The intercalating agents ethidium bromide, propidium iodide, and actinomycin D bind readily to ps-DNA, in some cases with greater affinity than to aps-DNA, whereas the nonintercalators bisbenzimidazole Hoechst 33258 (BBI-258) and DAPI form complexes with much reduced stability compared to aps-DNA[1,2,4,5,7,10,11,32] This difference can be exploited to distinguish between the two DNA conformations, either by direct measurements of the fluorescence or by analysis on native polyacrylamide gels followed by staining with BBI-258 and ethidium bromide. An example is

[32] J. B. Chaires, F. G. Loontiens, M. M. Garner, J. Klysik, R. M. Wadkins, and T. M. Jovin, in preparation.

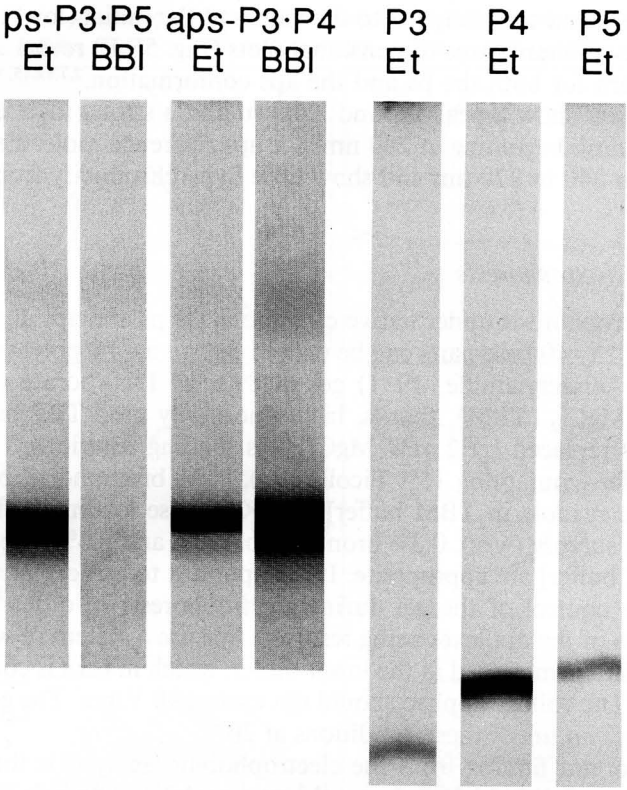


FIG. 6. Native gel electrophoresis and drug binding of oligonucleotides and their ps and aps duplexes. Gel electrophoresis under native conditions was carried out as described in the text. The amount of DNA applied to each lane was 0.2 nmol of strands. The gel was first stained with Hoechst 33258 (BBI-258, lanes denoted by BBI) followed by staining with ethidium bromide (lanes denoted by Et). The lanes with the single strands showed no fluorescence with BBI and are not included here. The digitized pictures of the fluorescent bands were obtained by illuminating the gel with a UV transilluminator and recording the images with a Series 200 slow-scan digital CCD camera (Photometrics, Tucson, AZ) and appropriate band-pass filters. (Data are from Klysik *et al.*[8])

shown in Fig. 6 for the ps-P3·P5 duplex (Fig. 1E) and its aps reference aps-P3·P4. It is apparent from the ethidium bromide-stained gel (Fig. 6, Et designated lanes) that the ps-P3·P5 duplex as well as the aps-P3·P4 reference molecules migrate as duplexes compared with the migration of the single-stranded P3, P4, and P5. No fluorescence is perceived on staining ps-P3·P5 with BBI-258, whereas the aps-P3·P4 reference shows the normal enhancement of fluorescence on drug binding (Fig. 6, BBI designated

lanes). BBI-258 has a strong preference for (dA·dT)-rich regions, and thus it is also excluded from the aps flanking regions of ps-P3·P5 and ps-P5·P6 in which d(G·C) base pairs predominate.

*Procedure: Double Staining with Hoechst 33258 (BBI-258) and Ethidium Bromide*

To reduce background staining it is important to use pure acrylamide and to electrophorese the gel for 60 min at 10 V/cm to remove traces of residual ammonium persulfate and acrylic acid prior to loading the samples. About 0.2–5 μg DNA per band can be loaded for the BBI-258 and ethidium bromide staining. The times for staining and destaining depend on the thickness of the gel and are given for a gel 1 mm thick. If the desired resolution is obtained, remove the gel carefully from the plate, immerse it in 0.15 μg/ml Hoechst 33258 (BBI-258) in TBM, and gently agitate for 5–20 min. Bands can be visualized by placing the gel on a standard transilluminator with UV light (~302 nm) or by illumination with a hand-held Hg-lamp (365 nm). The excitation maximum of BBI-258 is at 350 nm, and the emission maximum is at 465 nm. To photograph the gel use band-pass filters centered around the latter wavelength.

After destaining the gel in TBM without dye for about 30–60 min the gel is incubated in 1 μg/ml ethidium bromide in TBM for 10–20 min with gentle shaking. If the background is too high, destain for 20–30 min. Excitation is with a transilluminator at 302 nm. The emission maximum is at 610 nm. A suitable red cutoff filter can be used for photography.

*DNA Processing Enzymes and Chemical Probing*

Parallel-stranded DNA shows different substrate properties than B-DNA with several DNA processing enzymes (Table III). It is insensitive to the restriction enzymes *Dra*I, *Mse*I, and *Ssp*I and to degradation with pancreatic DNase I and *Escherichia coli* exonuclease III under standard conditions.[33] Chemical probing with a variety of reagents [osmium–pyridine, diethyl pyrocarbonate (DEPC), $KMnO_4$, and the phenanthroline–copper complex $(OP)_2Cu^+$] confirms that ps-DNA exists in an ordered duplex structure, but one that differs from aps-DNA[23] (Table III). For example, $(OP)_2Cu^+$ cleaves the aps but not the ps duplex, attesting to the specificity of this reagent (as well as of DNase I) for the minor groove geometry of B-DNA, a feature absent in the model of ps-DNA.[2,4,7]

[33] K. Rippe and T. M. Jovin, *Biochemistry* **28,** 9542 (1989).

TABLE III
SUBSTRATE PROPERTIES OF LINEAR PARALLEL-STRANDED DUPLEXES[a]

| Agent | NaCl[b] | Activity | | |
|---|---|---|---|---|
| | | ps | aps | ss |
| Restriction enzymes | | | | |
| *Dra*I | Low | − | +++ | ++ |
| *Mse*I | Low | − | +++ | − |
| *Ssp*I | Low | − | + | − |
| DNA nucleases | | | | |
| DNase I | Low | − | +++ | +++ |
| Exonuclease III | Low | − | ++ | +++ |
| Chemical reagents | | | | |
| Os,py | Low | − | − | ++ |
| | High | +++[c] | + | +++ |
| DEPC | Low | +[d] | +[d] | ++ |
| | High | + | + | + |
| $KMnO_4$ | Low | + | + | +++ |
| | High | +++ | ++ | +++ |
| $(OP)_2Cu^+$ | Low | − | ++[e] | + |

[a] Relative activities: +++, very high; ++, high; +, moderate; −, none or very low. Data for enzymatic activities were adopted from Rippe and Jovin[33] and those for chemical reagents are from Klysik *et al.*[23] obtained with the 25-bp linear ps and aps duplexes.[12] ss, Single strands or nonpairing combinations of oligonucleotides.

[b] In all cases 10 m*M* $MgCl_2$ was present. Low; <2 *M* NaCl; high, >4 *M* NaCl.

[c] High activity is attributable to reaction with single strands formed on dissociation of the duplex.

[d] Low reactivity was found, but the modification patterns of the same strand involved in ps or aps duplex formation are different.

[e] Preferred cutting sites are the TAT steps.

## Acknowledgments

We are indebted to N. B. Ramsing for long-standing participation and collaboration in many phases of this work. He is responsible for setting up the equation system for deriving the thermodynamic parameters in MATHEMATICA and for the graphic display program of secondary structures. We also thank our colleagues for critical reading of the manuscript.